

# FAST AND ACCURATE PREDICTIONS OF MEMS MICROMIRRORS NONLINEAR DYNAMIC RESPONSE USING DIRECT COMPUTATION OF INVARIANT MANIFOLDS

Andrea Opreni<sup>1</sup>, Alessandra Vizzaccaro<sup>2</sup>, Nicolò Boni<sup>3</sup>, Roberto Carminati<sup>3</sup>, Gianluca Mendicino<sup>3</sup>,  
Cyril Touzé<sup>4</sup>, and Attilio Frangi<sup>1</sup>

<sup>1</sup>Politecnico di Milano, ITALY,

<sup>2</sup>University of Bristol, UNITED KINGDOM,

<sup>3</sup>STMMicroelectronics, ITALY, and

<sup>4</sup>ENSTA Paris-CNRS-EDF-CEA-Institut Polytechnique de Paris, FRANCE

## ABSTRACT

The Direct Parametrisation of Invariant Manifolds (DPIM) is an innovative technique for Model Order Reduction (MOR) suitable for Micro-Electro-Mechanical Systems (MEMS) that operate at resonance, as most gyroscopes and scanning micromirrors. The computational performance and the sound mathematical foundation of the method allows identifying the nonlinear dynamic response of MEMS within short time spans and in a simulation-free context. For the first time, predictions of the method are compared with experimental data. Results highlight the remarkable industrial impact of the technique for accelerating the design of MEMS structures actuated at resonance.

## KEYWORDS

Invariant Manifold, Micromirrors, Piezoelectric, Model Order Reduction

## INTRODUCTION

Geometric [1] and material [2] nonlinearities represent the two main challenges associated to dimensionality reduction of finite element models of piezoelectric MEMS. The formers hinder the possibility to generate accurate reduced models using linear techniques as modal projection or the Proper-Orthogonal-Decomposition (POD) [3]. The latter, i.e. material nonlinearities associated to the nonlinear response of piezo materials when subjected to large potential biases, introduce hysteretic behaviour with respect to the applied voltage history and forces the solution of a coupled electromechanical problem to correctly estimate the response of the device [4]. As a consequence, the computational burden required to solve finite element models of piezo MEMS is not acceptable and often analytical or approximate techniques are used, which are however not accurate when highly nonlinear effects are present. In this framework, dimensionality reduction techniques represent a key tool for efficient and accurate estimation of the nonlinear dynamic response of structures subjected to strong nonlinearities [5].

Within the setting of MOR techniques for vibrating structures, two main classes of methods are present, i.e. linear and nonlinear techniques, the latter being the focus of the present work. Nonlinear techniques aim at defining a nonlinear relationship between the original coordinates of the system [6], i.e. nodal displacements of a finite element model, and the coordinates of the reduced dynamics, hence providing higher accuracy with subspaces of smaller

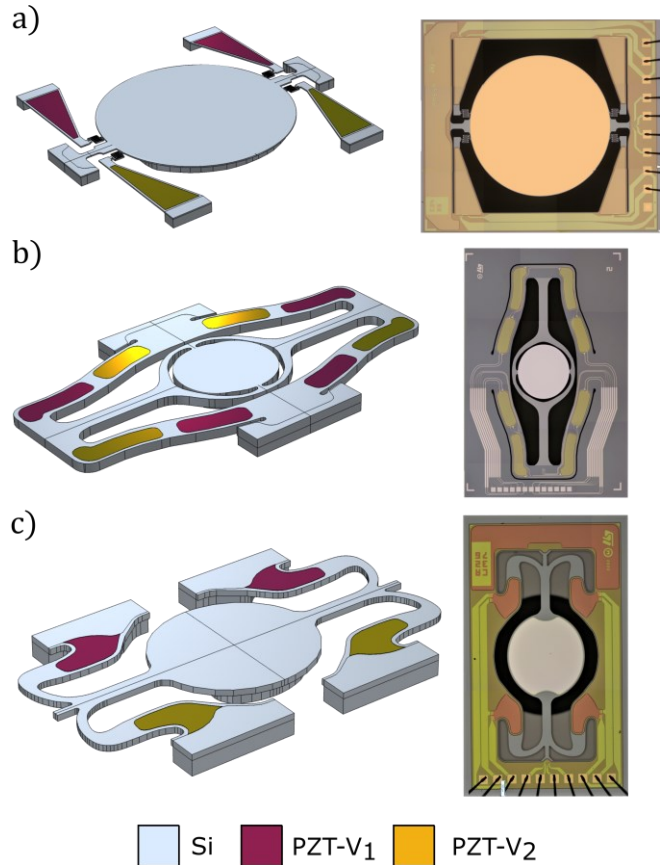


Figure 1: geometries and optical microscope pictures of the tested devices: mirror 1 (a), mirror 2 (b), and mirror 3 (c). Grey colour is used for silicon. Red and yellow colours are used to highlight the PZT actuation patches. The two colours are used to distinguish between actuation groups 1 and 2.

dimension compared to linear techniques [7]. In this setting, methods as the Direct Normal Form (DNF) [8-9], which is a special declination of the broader class of DPIM methods [10], are showing unprecedented speed and accuracy for developing reduced models of vibrating structures since they prove able to efficiently address geometric nonlinearities. In the present work, a high order DNF combined with the piezoelectric modeling strategy presented in [11] is applied to efficiently model piezoelectric MEMS actuated at large rotation angles. Comparison with experimental data show the remarkable gain in adopting nonlinear reduction techniques for fast and accurate prediction of the nonlinear dynamic response of piezo MEMS micromirrors excited at large rotation amplitudes.

## MODEL DESCRIPTION

This work addresses structures actuated at resonance with large displacements, hence the governing equation is the conservation of linear momentum in a finite elasticity framework:

$$\int_{\Omega} \rho \dot{\mathbf{u}} \cdot \mathbf{w} d\Omega + \int_{\Omega} \mathbf{T} : \delta \mathbf{e} d\Omega = 0 \quad \forall \mathbf{w} \in C(\mathbf{0}), \quad (1)$$

with  $\rho$  density,  $\mathbf{u}$  displacement,  $\mathbf{w}$  test function belonging to the space  $C(\mathbf{0})$ , i.e. space of functions that vanish on the boundary where Dirichlet boundary conditions on the displacement field are imposed.  $\mathbf{T}$  is the second Piola-Kirchhoff stress tensor, and  $\delta \mathbf{e} = (\nabla \mathbf{w} + \nabla^T \mathbf{w} + \nabla^T \mathbf{u} \cdot \nabla \mathbf{w} + \nabla^T \mathbf{w} \cdot \nabla \mathbf{u})/2$  is the first variation of the Green-Lagrange strain tensor  $\mathbf{e}$ .  $\Omega$  is the structure domain. All quantities are defined in material configuration.

Piezoelectric effect is added using the modeling strategy proposed in [11-12]. Under the assumption of large actuation voltages inelastic strains  $\mathbf{S}^p$  are mostly caused by electrostriction in materials with strong electrostrictive coefficients as lead zirconate-titanate as PZT:

$$\mathbf{S}^p = \mathbb{Q} : (\mathbf{p} \otimes \mathbf{p}), \quad (2)$$

with  $\mathbb{Q}$  electrostrictive tensor, and  $\mathbf{p}$  polarization field. We can then decouple stresses as:

$$\mathbf{T} = \mathbf{T}^e - \mathbf{T}^p, \quad (3)$$

with:

$$\mathbf{T}^e = \mathbb{A} : \mathbf{e}, \quad \mathbf{T}^p = \mathbb{A} : (\mathbb{Q} : (\mathbf{p} \otimes \mathbf{p})), \quad (4)$$

where  $\mathbb{A}$  is the fourth order elasticity tensor. The resulting equation that governs the problem is:

$$\int_{\Omega} \rho \dot{\mathbf{u}} \cdot \mathbf{w} d\Omega + \int_{\Omega} \mathbf{e} : \mathbb{A} : \delta \mathbf{e} d\Omega = \int_{\Omega_p} (\mathbb{Q} : (\mathbf{p} \otimes \mathbf{p})) : \mathbb{A} : \delta \mathbf{e} d\Omega \quad \forall \mathbf{w} \in C(\mathbf{0}), \quad (5)$$

with  $\Omega_p$  volume of the piezoelectric material. We now introduce a finite element discretisation of the problem and we add damping to the system, hence retrieving the following system of coupled differential equations [12]:

$$\mathbf{M}\ddot{\mathbf{U}} + \mathbf{C}\dot{\mathbf{U}} + \mathbf{K}\mathbf{U} + \mathbf{G}(\mathbf{U}, \mathbf{U}) + \mathbf{H}(\mathbf{U}, \mathbf{U}, \mathbf{U}) = \mathbf{F}_{\text{piezo}}(\mathbf{p}, \mathbf{U}, t), \quad (6)$$

with  $\mathbf{M}$  mass matrix,  $\mathbf{C}$  damping matrix,  $\mathbf{K}$  stiffness matrix,  $\mathbf{G}$  quadratic nonlinearity tensor,  $\mathbf{H}$  cubic nonlinearity tensor,  $\mathbf{F}_{\text{piezo}}(\mathbf{p}, \mathbf{U}, t)$  piezoelectric force,  $t$  time, and  $\mathbf{U}$  nodal displacement vector. In the remainder of the work we neglect displacement dependence of the piezoelectric force since  $\mathbf{F}_{\text{piezo}}(\mathbf{p}, \mathbf{U}, t) \approx \mathbf{F}_{\text{piezo}}(\mathbf{p}, t)$ . The polarization is assumed known a priori using experimental data collected on the piezoelectric patches and it is used as input of the model to avoid solving the coupled problem as done in [11].

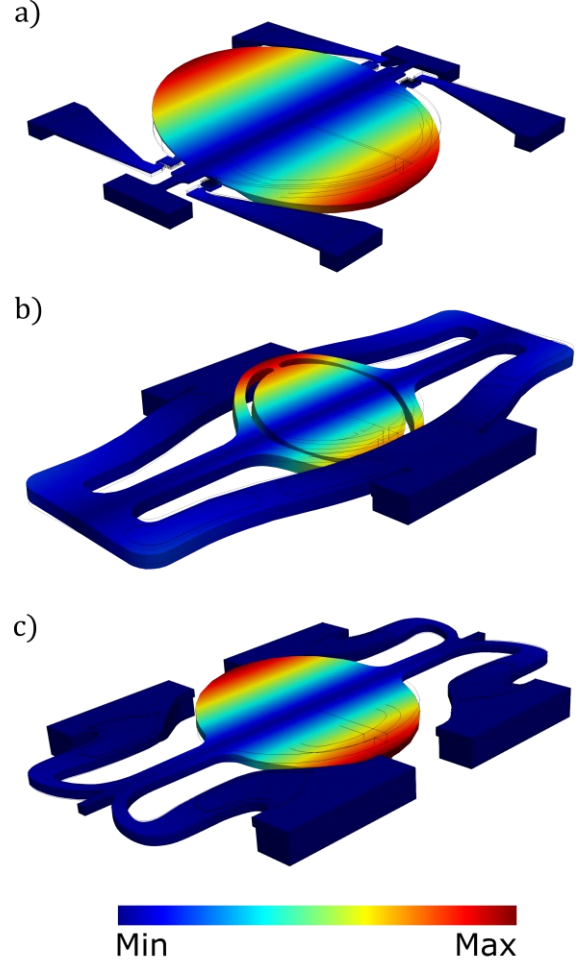


Figure 2: displacement field associated to the torsional eigenmodes of the tested structures. Mirror 1 has a resonance frequency of 1950 Hz (a), Mirror 2 has a resonance frequency of 25000 Hz (b), and mirror 3 has a resonance frequency of 28000 Hz (c).

## DIMENSIONALITY REDUCTION

The DPIM is applied to reduce the left hand side of Eq. (6) by parametrising the system motion along the invariant manifold of the drive mode, which is an approximation of the unique spectral submanifold [13-14]. To this aim, a nonlinear change of coordinates between displacement  $\mathbf{U}$ , velocity  $\mathbf{V}$ , and the normal coordinates  $\mathbf{z}$  of the reduced model is introduced:

$$\mathbf{U} = \Psi(\mathbf{z}), \quad \mathbf{V} = \mathbf{Y}(\mathbf{z}). \quad (7)$$

$\Psi(\mathbf{z})$  and  $\mathbf{Y}(\mathbf{z})$  are polynomial nonlinear coordinate change. The reduced dynamics onto the manifold is then defined as:

$$\dot{\mathbf{z}} = \mathbf{f}(\mathbf{z}), \quad (8)$$

where  $\mathbf{f}(\mathbf{z})$  is a polynomial law estimated during the reduction procedure. Eq. (8) allows defining the time derivatives of displacement and velocity as:

$$\dot{\mathbf{U}} = \nabla_{\mathbf{z}} \Psi(\mathbf{z}) \mathbf{f}(\mathbf{z}), \quad \dot{\mathbf{V}} = \nabla_{\mathbf{z}} \mathbf{Y}(\mathbf{z}) \mathbf{f}(\mathbf{z}). \quad (9)$$

Substitution of Eq. (7) and (9) in the first order formulation of (6) yields a set of algebraic homological equations that are solved to retrieve mappings  $\Psi(\mathbf{z})$  and  $\mathbf{Y}(\mathbf{z})$  and the reduced dynamics law  $\mathbf{f}(\mathbf{z})$ . Forcing is then added to the system by projecting it on the drive mode. The resulting reduced model upon conversion to a second order formulation is then obtained as:

$$\ddot{R} + \frac{\Omega_0}{Q} \dot{R} + \Omega_0^2 R + f(R, \dot{R}) = \sum_{i=1}^{N_p} P_i^2(t) F_i^{\text{piezo}}, \quad (10)$$

with  $R$  real-valued normal coordinate provided by the realification of  $\mathbf{z}$ ,  $\Omega_0$  resonance frequency of the drive mode,  $Q$  quality factor,  $f(R, \dot{R})$  nonlinear restoring force estimated by the parametrisation procedure,  $P_i$  average polarization value of the  $i$ -th piezoelectric patch, and  $F_i^{\text{piezo}}$   $i$ -th modal piezoelectric force.  $N_p$  is the total number of piezoelectric patches. The analysis is then reduced to solving Eq. (10), which in absence of internal resonances [15] is a single degree of freedom differential equation, and to reconstructing the physical displacement with Eq. (7). The main advantage of this technique is that it allows addressing non-resonant coupling between drive and spurious modes. The right hand side of Eq. (6) is treated by projecting the forcing term onto the drive mode linear modal subspace. This approximate technique holds well for systems excited at large amplitudes and subjected to small forcing values, which is typical in MEMS structures. The resulting reduced model fully captures the main nonlinear dynamic features of the drive mode, and it provides an accurate estimation of the displacement field. Furthermore, the method is simulation-free, hence it does not require sample solutions to reduce the system dimension as for instance required by the POD [3]. This in turns makes the DPIM the most accurate and efficient dimensionality reduction technique for predicting the nonlinear dynamic response of resonating structures.

## DEVICE OVERVIEW, FABRICATION, AND TESTING

The presented reduction strategy is applied to study the nonlinear dynamic response of three MEMS micromirrors developed by STMicroelectronics<sup>TM</sup>. Geometry and optical microscope images of the three devices are reported in Fig. 1. All devices are made in single crystal silicon with the [100] orientation aligned along the main axis of the reflective surfaces suspension springs. Mirror 1 reported in Fig. 1(a) features a 3000  $\mu\text{m}$  diameter reflective surface. Actuation is performed using four PZT patches deposited with the Petra<sup>TM</sup> process. Mirror 2 is reported in Fig. 1(b) and has a reflective surface with a diameter of 1600  $\mu\text{m}$ . It is actuated using eight PZT patches deposited on the outer side of its gimbal structure. Mirror 3 is reported in Fig. 1(c) and it features four PZT patches as mirror 1. It has a reflective surface of 1100  $\mu\text{m}$ . Adopted material properties for silicon and PZT are taken from [12].

All devices are actuated at their first torsional mode, at a frequency of 1950 Hz, 25000 Hz, and 28000 Hz respectively. The displacement fields associated to the torsional modes of the devices are reported in Fig. 2.

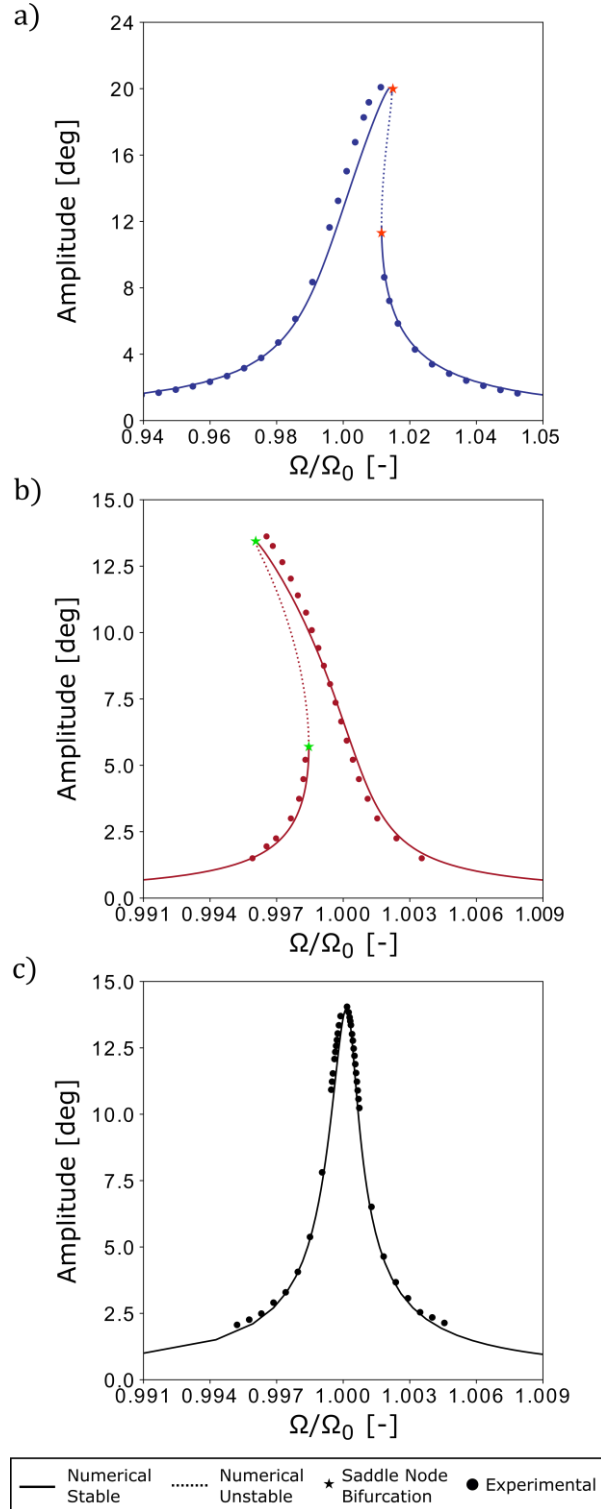


Figure 3: mirror 1 (a), mirror 2 (b), and mirror 3 (c) frequency response curves.

Actuation is achieved by grouping the piezoelectric patches in two actuation sets and the two groups are actuated with unipolar potential laws  $V_1 = (V_0/2)(1 + \cos(\omega t))$  and  $V_2 = (V_0/2)(1 - \cos(\omega t))$  to avoid polarization switch. Quality factors of the devices are obtained from experimental data using the procedure detailed in [16] and they are reported in Table 1, together with actuation voltages  $V_0$ .

Table 1: quality factors measured from experimental data and actuation voltage amplitudes  $V_0$  for the three devices.

	Mirror 1	Mirror 2	Mirror 3
Q [-]	105	1092	800
$V_0$ [V]	20	30	20

The input signal used to actuate the devices is obtained using the function generator “Agilent 33521 A.”. During actuation the opening angle is measured using a He-Ne laser. The reflected beam collides on a detector and the line spanned on the detector provides a measure of the opening angle of the device. The experiment is performed in frequency control. Each device is tested both with an upward and a downward frequency sweep.

## RESULTS

The DPIM is applied to parametrise the system motion along the invariant manifold associated to the torsional mode of the devices using an order 9 asymptotic expansion with real normal form style [10]. The piezoelectric forcing is computed using the procedure reported in [11], i.e. we measured the average polarization field of the piezoelectric patches for the tested polarization histories and we used it as input for the model. Polarization measures were performed using a Sawyer-Tower circuit. Only the first harmonic term of the force is used since higher order terms provided no benefit. Numerical solution of the reduced model is performed with the continuation package BifurcationKit [17]. The comparison between experimental data and numerical simulations is reported in Fig. 3. Results highlight the excellent agreement between simulated curves and experiments, hence illustrating the benefits of adopting nonlinear reduction techniques for modeling MEMS resonant structures. The total analysis time to derive the reduced models and simulate the nonlinear dynamic response of the systems is smaller than 10 minutes for all finite element models combined.

## CONCLUSIONS

We leveraged nonlinear reduction methods based on the invariant manifold theory to predict in a data-free method the nonlinear dynamic response of MEMS micromirrors. The comparison between experimental and numerical data highlighted the ability of the technique to perfectly identify the nonlinear dynamic response of structures excited at resonance. Furthermore, the unprecedented numerical performance of the method allows exploiting it during the design stage of MEMS components to identify structural nonlinearities.

## REFERENCES

[1] C. Touzé, et al. Model order reduction methods for geometrically nonlinear structures: a review of nonlinear techniques. *Nonlinear Dynamics*, vol. 105, pp. 1141-1190, 2021

[2] A. Opreni, et al. Modeling Material Nonlinearities in Piezoelectric Films: Quasi-Static Actuation. *Proceeding of the 2021 IEEE 34th International Conference on Micro Electro Mechanical Systems (MEMS)*, pp. 85-88, 2021

[3] G. Gobat, et al. Reduced order modeling of nonlinear microstructures through Proper Orthogonal

Decomposition. *arXiv*, 2109, 2021

[4] P. Fedeli et al. Phase-field modeling for polarization evolution in ferroelectric materials via an isogeometric collocation method. *Computer Methods in Applied Mechanics and Engineering*, vol. 351, pp. 789-807, 2019.

[5] A. Vizzaccaro et al. Non-intrusive reduced order modelling for the dynamics of geometrically nonlinear flat structures using three-dimensional finite elements. *Computational Mechanics*, vol. 66(6), pp. 1293-1319, 2020

[6] A. Vizzaccaro et al. Comparison of nonlinear mappings for reduced-order modelling of vibrating structures: normal form theory and quadratic manifold method with modal derivatives. *Nonlinear Dynamics*, vol. 103(4), pp. 3335-3370, 2021

[7] M. Amabili and C. Touzé. Reduced-order models for nonlinear vibrations of fluid-filled circular cylindrical shells: comparison of POD and asymptotic nonlinear normal modes methods. *Journal of fluids and structures*, vol. 23(6), pp. 885-903, 2007

[8] A. Vizzaccaro et al. Direct computation of nonlinear mapping via normal form for reduced-order models of finite element nonlinear structures. *Computer Methods in Applied Mechanics and Engineering*, vol. 384, sp. 113957, 2021

[9] A. Opreni et al. Model order reduction based on direct normal form: application to large finite element MEMS structures featuring internal resonance. *Nonlinear Dynamics*, vol. 105, pp. 1237-1272, 2021

[10] A. Vizzaccaro et al. Higher order direct parametrisation of invariant manifolds for model order reduction of finite element structures: application to large amplitude vibrations and uncovering of a folding point. *arXiv*, 2109.10031, 2021

[11] A. Frangi et al. Nonlinear response of PZT-actuated resonant micromirrors. *Journal of Microelectromechanical Systems*, vol. 29(6), pp. 1421-1430, 2020

[12] A. Opreni et al. Analysis of the nonlinear response of piezo-micromirrors with the harmonic balance method. *Actuators*, vol. 10(2), sp. 21, 2021

[13] S. Jain and G. Haller, How to compute invariant manifolds and their reduced dynamics in high-dimensional finite element models. *Nonlinear dynamics*, in press, 2021

[14] G. Haller and S. Ponsioen, Nonlinear normal modes and spectral submanifolds: existence, uniqueness and use in model reduction. *Nonlinear Dynamics*, vol. 86, pp. 1493-1534, 2016

[15] G. Gobat et al. Reduced order modelling and experimental validation of a MEMS gyroscope test-structure exhibiting 1: 2 internal resonance. *Scientific Reports*, vol. 11(1), pp. 1-8, 2021

[16] Davis W.O. Measuring Quality Factor From a Nonlinear Frequency Response With Jump Discontinuities. *Journal of Microelectromechanical Systems*, vol. 20, pp. 968-975, 2011

[17] R. Veltz. BifurcationKit.jl, <https://hal.archives-ouvertes.fr/hal-0290234>, 2020.

## CONTACT

\* A. Opreni, tel: +39-3493776864; andrea.opreni@polimi.it